

## JAMESON AND HOFFERT: PHASE AND AMPLITUDE CONTROL OF HIGH-POWER RF SYSTEMS 205

### FAST AUTOMATIC PHASE AND AMPLITUDE CONTROL OF HIGH-POWER RF SYSTEMS\*

Robert A. Jameson and William J. Hoffert

Los Alamos Scientific Laboratory  
Los Alamos, New Mexico

#### Summary

Recent progress in the design and testing of the fast feedback rf control system being developed for the Los Alamos Meson Physics Facility (LAMPF) proton linac is reviewed. Closed-loop rf phase control with correction bandwidths greater than 200 kHz is demonstrated using a coaxitron power amplifier driving a full-scale accelerator structure. Proposed experimental studies to determine control characteristics, synthesize closed-loop amplitude control systems, and study phase-amplitude interactions in 1.25-MW, 6% duty factor klystron, triode, and crossed-field amplifier systems are outlined. Extremely phase-stable frequency sources have been developed to supply reference signals at 201.25 MHz and 805 MHz. The design and testing techniques used to verify phase stability and mutual coherence of the harmonically related outputs are summarized.

#### RF Phase Control

The tolerance<sup>1, 2</sup> on the phase of the rf field in the LAMPF linac is about  $\pm 2^\circ$ . This tolerance must be maintained during corrections for beam loading. The feasibility of such control has been demonstrated with the 805-MHz system shown in Fig. 1, using a coaxitron high-power amplifier with a  $\pi$ -mode cloverleaf accelerator structure as a resonant load.

The coaxitron was operated at 20 kV during this experiment to insure reliable operation; about 400-kW drive was provided to the cloverleaf--slightly above rated power for this particular structure. The cloverleaf tank will be replaced by a side-coupled  $\pi/2$ -mode structure in the final machine; some simulation of the mode spacing to be expected from the side-coupled tank was obtained by driving in the center cell and sensing the tank field in a cell halfway between the center and the end.

The block diagram of the closed-loop system is shown in Fig. 2. The open-loop phase modulation transfer functions were measured experimentally and are shown in terms of frequency, (Hz), scaled by  $10^4$ . The noise input, N, was imposed by adding a sinusoidal "noise" modulation to the bias voltage,  $\Delta V_b$ , and represents a phase disturbance in the power amplifier such as the change in transit time when the power output is increased to compensate for beam loading. The noise, Q, represents a disturbance in the accelerator cavity, such as beam loading. It is imposed directly on the tank sensing line, using another varactor phase shifter, and is a pessimistic representation in that the filtering effect of the cavity is not considered. The circuitry in the phase error detector and

compensating elements was built around integrated circuit operational amplifiers.

The transfer functions which explain the operation of the system are shown in Fig. 3. For example, with a fixed phase reference,  $\Delta\phi_p$ , the transfer function,  $\Delta\phi_e/N$ , shows how much of the noise input, N, shows up as phase error on the tank field as a function of the frequencies contained in N. In this case, attenuation of at least 10 dB is provided at all frequencies.  $\Delta\phi_e/Q$  demonstrates a correction bandwidth of at least 200 kHz.

Further details on this experiment are contained in Reference 3. Refinements will be made during experiments with additional types of rf amplifiers as outlined below.

#### RF Amplitude and Combined Phase-Amplitude Control

The control characteristics of the various types of high-power rf amplifier systems under evaluation at LASL<sup>4</sup> have been estimated for design purposes from detailed measurements of R&D accelerator structures and test amplifier systems, including a 100-kW (peak output) klystron and crossed-field amplifier, and a 3% duty factor, 1-MW coaxitron.<sup>5</sup>

These measurements will be expanded during tests of full power 1.25-MW versions of the three amplifier types. Hard-tube modulators have been developed, with high-speed interface units<sup>6</sup> suitable for fast rf amplitude control. Open-loop measurements have been completed and closed-loop amplitude control experiments should begin soon. Closed-loop experiments are also in progress using rf drive modulation to control amplitude; this approach will be used with the 1.25-MW klystron amplifier. The initial amplitude control experiments will probe the frequency response limits of the hardware and the effects of time delays in the system. Combined phase and amplitude control will then be attempted, to determine whether the coupling between the two loops will be a problem. The interaction is not expected to be serious; however, the final design may have to incorporate some kind of isolation, such as a difference in bandwidth. It appears at present that practicality would dictate that the amplitude control loop be made slower.

#### Phase Stable Reference Frequency Generation<sup>2</sup>

#### Accelerator Phase Tolerance

The remainder of this paper treats the development of the phase reference, or master oscillator, for the LAMPF linac, which operates at two harmonically related frequencies, 201.25 MHz and 805 MHz. As mentioned earlier, the basic tolerance on variations of the phase of the rf field

\* Work performed under the auspices of the U. S. Atomic Energy Commission.

between adjacent accelerator tanks is about  $\pm 2^\circ$ . This tolerance was derived from beam dynamical studies of particle motion through a typical accelerator; the method consisted of a correlation of phase emittance statistics at various points in the machine with the statistics of tank-to-tank amplitude and phase errors. This specification is refined to say that the phase control system shall reduce the effect of all systematic disturbances to less than  $\pm 2^\circ$ , and that the standard deviation of all random noise in the system shall be less than  $\pm 2/3^\circ$ , which reduces the probability of random disturbances greater than  $2^\circ$  to 0.3%. The specification on the mutual coherence, or harmonic relationship, between the 201.25 and 305 MHz references is of the same order. The time period over which this stability is of interest is from 1-2 ms, corresponding to maximum rf pulse lengths, down to fractions of a microsecond, corresponding to accelerator structure mode separation and control loop bandwidths.

These tolerances are on tank-to-tank relative phase and coherency at the frequency transition, not on absolute phase. That is, particle acceleration would not be affected by a phase drift as long as the whole machine could track without exceeding the relative tolerance. However, an extremely stable reference system to which each amplifier system is compared has many advantages, among them non-propagation of errors along the machine and the freedom to design the control loop to do its primary job of correcting disturbances originating within the loop without concern for fluctuations in the reference. The following paragraph develops the specifications for such a source.

#### Reference Generator Phase Tolerance

First of all, the reference generator should be capable of producing an accelerator cavity field which, in the absence of outside disturbances, remained within tolerance. Thus, the field tolerances must be interpreted from the viewpoint of the generator output, and in such a form that experimental verification of the stability is possible.

If a practical oscillator oscillating at a constant mean frequency but containing random instantaneous phase or frequency fluctuations is compared to a perfect oscillator at the mean frequency, the rms phase error in a period  $\tau$  can be expressed in the time domain as

$$\sigma_\theta(\tau) = \sqrt{E\left[\left\{\dot{\theta}(t) \otimes p_\tau\left(t + \frac{\tau}{2}\right)\right\}^2\right]} \quad (1)$$

where  $E[\ ]$  denotes the "statistical average";  $\dot{\theta}(t)$  is the instantaneous frequency fluctuation of the imperfect oscillator; and  $\otimes$  indicates the convolution of  $\dot{\theta}(t)$  with a rectangular pulse,  $p_\tau(t)$  from  $-\tau/2 \leq t \leq \tau/2$ .

By using Fourier transforms, the right side of Eq. (1) can be expressed in the frequency domain as

$$\sigma_\theta(\tau) = \tau \sqrt{\frac{1}{2\pi} \int_{-\infty}^{\infty} S_{\dot{\theta}}(\omega) \left(\frac{\sin \omega\tau/2}{\omega\tau/2}\right)^2 d\omega} \quad (2)$$

where the mean-square spectral density,  $S_{\dot{\theta}}(\omega)$ , of the instantaneous frequency fluctuations is weighted

by the filtering effect of the time interval,  $\tau$ , over which the instabilities have cumulated their effect.  $S_\theta(\omega)$ , the mean-square spectral density of the instantaneous phase fluctuations, is related to  $S_{\dot{\theta}}(\omega)$  by  $S_\theta(\omega) = \omega^2 S_{\dot{\theta}}(\omega)$ . Equation (2) is important, because  $S_{\dot{\theta}}(\omega)$  and  $S_\theta(\omega)$  are functions which can be quite readily measured.

The smoothing effect of a filter on Eq. (2) is as follows, where  $H(j\omega)$  characterizes the filter:

$$\sigma_\theta(\tau) = \sqrt{\frac{1}{\pi} \int_{-\infty}^{\infty} S_\theta(\omega) (1 - \cos \omega\tau) |H(j\omega)|^2 d\omega} \quad (3)$$

If the accelerator structure is treated as a singly resonant cavity, its filter function can be written

$$H(j\Delta\omega) \cong \frac{1}{1 + j\Delta\omega/\Delta\omega_{\frac{1}{2}}} \quad (4)$$

where  $\Delta\omega$  is a small frequency shift from the cavity resonant frequency and  $\Delta\omega_{\frac{1}{2}}$  is the half-power off-resonance frequency.

Letting  $S_\theta(\Delta\omega)$  be constant, Eq. (3) can then be solved in terms of the specification on the accelerator field to determine the maximum  $S_\theta(\omega)$  permissible in the reference source for measuring times in the range of interest.

$$\sqrt{S_\theta}_{\max} = \frac{\sigma_\theta^2(\tau)}{\Delta\omega_{\frac{1}{2}} \left(1 - e^{-\Delta\omega_{\frac{1}{2}}\tau}\right)} \quad (5)$$

$$S_\theta_{\max} = \left[ \frac{(0.667)^2}{4 \times 10^4 (1 - e^{-8.17 \times 10^4 \tau})} \frac{(\text{deg})^2}{\text{cps}} \right]^{\frac{1}{2}} \\ \cong 3.34 \times 10^{-3} \frac{\text{deg}}{\sqrt{\text{cps}}} \quad \left| \tau > 10^{-5} \text{ sec} \right. \quad (6)$$

for a cavity with a loaded  $Q = 10,000$  at 805 MHz.

#### Practical Realization

A practical reference must contain an oscillator, capable of the stability indicated above, operating either at the desired frequency or at another frequency and followed by multipliers or other signal conditioning to reach the desired frequency. Based on extensions of the above ideas, it has been decided that the best approach for the LAMPF system is to use a very stable quartz crystal oscillator in the 5-MHz region as the basic oscillator, followed by multiplication to 201.25 and 305 MHz in a series string. Commercial quartz oscillators are available which exhibit extremely good short-term stability and long-term stability approaching that of atomic standards. The  $S_\theta(\omega)$  characterizing the 805-MHz reference will contain the input noise to the multiplier chain multiplied by the ratio of the output-to-input frequencies, plus any additional noise added by the multiplier itself.

Three types of multipliers are under consideration; vacuum tube, transistor-varactor, and step-recovery diode. In the tube multiplier, diode bridge doubler stages are used, followed by two-stage tuned Class A amplifiers to restore the

power level. This approach reduces (by ~ 20 dB) the tendency of ordinary Class C doubler outputs to exhibit input frequency AM on the output. The varactor multiplication per stage is also low, X3, to minimize the stability-degrading effects of high-order multiplication. A combination of lumped and distributed circuitry is used, with special attention to component placement, shielding, grounding, component and load sensitivity, reliability, etc. Output levels are approximately one watt. Figure 4 is a photo of some of the tube multiplier stages. Tests on the tube multiplier are summarized below; the other versions will be ready for testing in the near future.

Experimental Verification of Stability

The phase spectral density,  $S_{\theta}(\omega)$ , at the desired frequency can be measured as shown in Fig. 5, by driving identical multiplier chains with a common source, phase comparing the outputs, analyzing the spectral content of the result, and assigning the noise on an rms basis to each multiplier. The phase bridge output is given by

$$\frac{E_{\theta}(t)}{\theta(t)} \cong \frac{Gk(2E^2)^{n/2}}{57.3} = \xi \frac{\text{volts}}{\text{deg}} \quad (7)$$

where G is the comparator gain and k and n are the detector efficiency and detection law, respectively. Treating the analyzer filter as singly resonant with bandwidth =  $\Delta f_{a1}$  and the recorder time constant as  $\tau_r$ , the spectral density  $S_{\theta}(\omega)$  for each multiplier can be calculated from the recorded voltage,  $E_a$ , using Eq. (5), assuming a constant  $S_{\theta}(\omega)$  over the analyzer bandwidth:

$$\sqrt{S_{\theta}}_{\text{max}} = \frac{E_a (\text{peak factor})}{\sqrt{2\xi} \sqrt{\Delta f_{a1}(1 - e^{-\Delta\omega a_1 \tau_r})}} \frac{\text{deg}}{\sqrt{\text{cps}}} \quad (8)$$

The peak factor weights the statistics of the phase noise against the analyzer meter, which is calibrated to read the rms value of a pure sine wave. This factor is approximately 1.13 for gaussian noise in the analyzer band. In most cases,  $\tau_r$  is long and the exponential can be ignored. The  $\sqrt{2}$  assigns half the noise power to each chain.

The factor  $\xi$  can be determined directly using the manual phase shifter. The hybrid ring phase bridge provides inherent discrimination against AM on the multiplier outputs (usually very small anyway) and provides self-error evaluation when one signal is split between both inputs.

Measurements of the tube multipliers operating on batteries demonstrated AM levels of greater than 110 dB below the carrier at 60 Hz from the carrier, and greater than 120 dB between 100 Hz and 1.5 MHz from the carrier.

Figure 6 is a measurement of  $S_{\theta}(\omega)$  at 805 MHz for the tube multipliers using dc supplies operating from the ac line and driving with a simple, relatively unstable crystal oscillator. The specification of Eq. (6) is met down to 500 Hz from the carrier;  $S_{\theta}(\omega)$  falls rapidly out to about 500 kHz and then levels off. A large part of the noise near the carrier is due to the crystal oscillator and power supply ripple; a source such as the Hewlett-Packard Model 107B and the refined con-

struction techniques of a finalized design should result in a one-watt source that far exceeds the stability required by (6). Such a cushion will ease the problem of amplification and distribution of the reference along the machine.

Mutual Coherence

The 805-MHz output of the multiplier chain is derived from the 201.25-MHz stage; thus, the stability at 201.25-MHz is at least as good as that demonstrated in Fig. 5. At the frequency transition in the linac, the mutual coherence between these harmonically related frequencies is of utmost importance. A theoretical basis for the subject of coherency has recently been developed;<sup>9</sup> it suffices here to outline a measurement method and some preliminary results. The method is the same as that shown by Fig. 4 and Eq. (8), except with the hybrid ring replaced by a matched, resistive tee to which the 201.25 and an attenuated 805-MHz output are applied. The resulting mixture is split in another tee and detected in the same manner. The  $\xi$  factor of Eq. (7) is found directly with a manual phase shifter in the 805-MHz input. Preliminary measurements with the tube multiplier chains indicate that the spectral density of phase fluctuations from mutual coherency of the 201.25 and 805-MHz outputs is less than  $10^{-3}$  deg/ $\sqrt{\text{cps}}$  from 250 Hz to 1.5 MHz away from the carrier.

Conclusions

The above is a brief sketch of the considerations necessary to generate a stable phase reference for a particle accelerator with stringent tolerances such as the proposed LAMPF proton linac. The feasibility of such a source has been demonstrated. Further experiments are planned to refine construction and measurement techniques.

References

1. R. A. Jameson, T. F. Turner, and N. A. Lindsay, "Design of the RF Phase and Amplitude Control System for a Proton Linear Accelerator," IEEE Trans. on Nucl. Sci., Vol. NS-12, No. 3, June, 1965.
2. R. A. Jameson, "Analysis of a Proton Linear Accelerator RF System and Application to RF Phase Control," LA-3372, Los Alamos Scientific Laboratory, Los Alamos, New Mexico, 1965.
3. R. A. Jameson, W. J. Hoffert, and N. A. Lindsay, "Fast RF Control Work at LASL," Proc. of the 1966 Linac Accelerator Conference, Oct. 3-7, 1966, LA-3609, Los Alamos Scientific Laboratory, Los Alamos, New Mexico, pp. 460-466.
4. D. C. Hagerman, "High Duty Factor RF Sources at 800 MHz," Proceedings this conference.
5. "Quarterly Status Reports on the Medium Energy Physics Program for Periods Ending April 30, July 31, and October 31, 1966," LA-3521-MS, LA-3587-MS, and LA-3419-MS, Los Alamos Scientific Laboratory, Los Alamos, New Mexico.
6. R. P. Severns, T. F. Turner, and A. R. Koelle, "Crossing High-Voltage Interfaces with Large

- Bandwidth Signals," Proceedings this conference.
7. E. J. Baghdady, R. N. Lincoln, and B. D. Nelin, "Short-Term Frequency Stability: Characterization, Theory, and Measurement," IEEE-NASA Symposium on Short-Term Frequency Stability, NASA-SP-80, Nov., 1964.
  8. J. R. Parker, private communication. See also Reference 7 for discussion of peak factors.
  9. E. J. Baghdady, EXCERPTS FROM ELEMENTS OF SIGNAL THEORY, Chap. II, to be published (private communication).

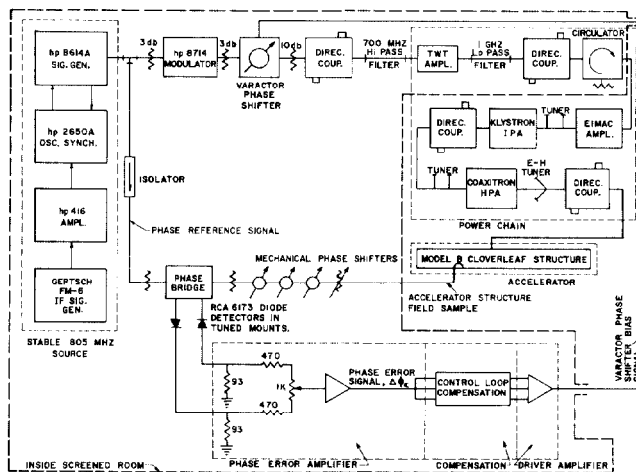


Fig. 1. 805-MHz rf phase control system for an accelerator module.

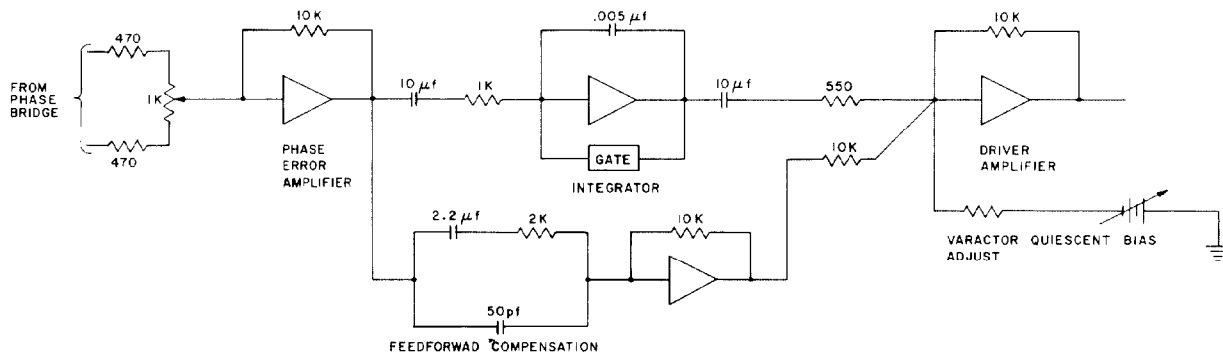
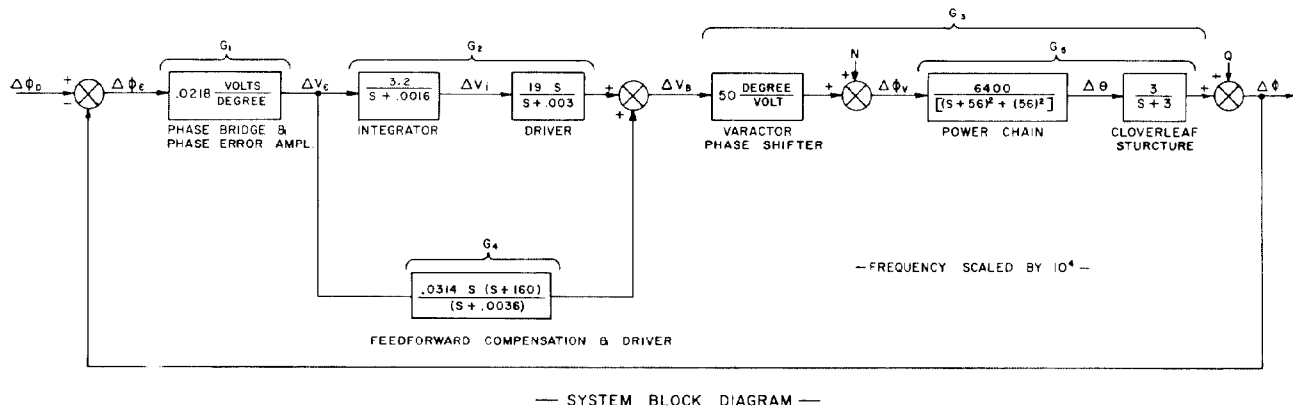


Fig. 2. Closed-loop phase control experiment.

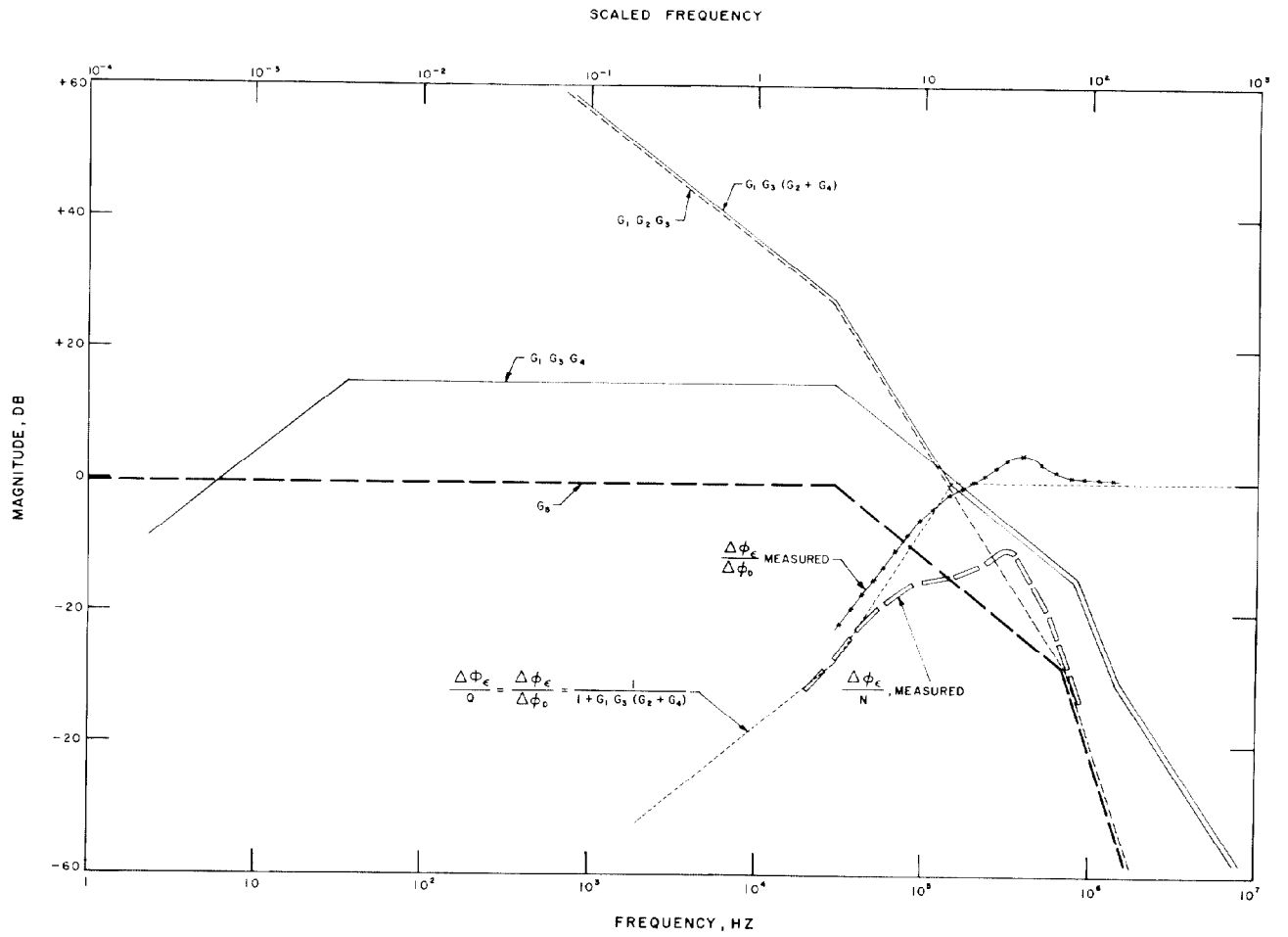


Fig. 3. Transfer functions for the rf phase control loop in Fig. 2.

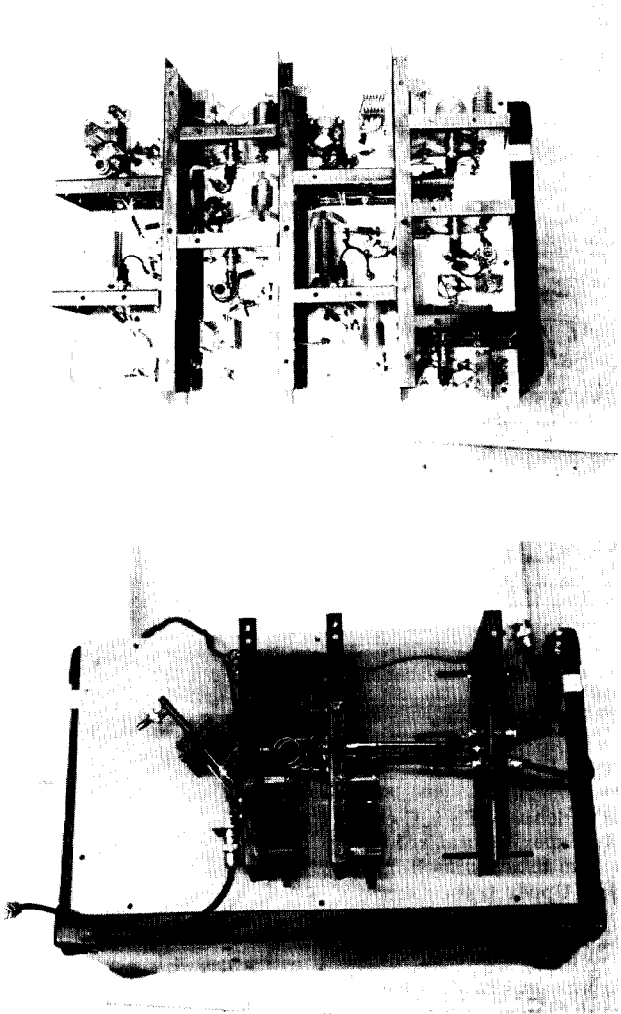


Fig. 4. Construction techniques used for an experimental vacuum tube multiplier chain. Top: 6.283 MHz to 100.625 MHz doubler stages. Bottom; 201.25 MHz to 402.5 MHz doubler.

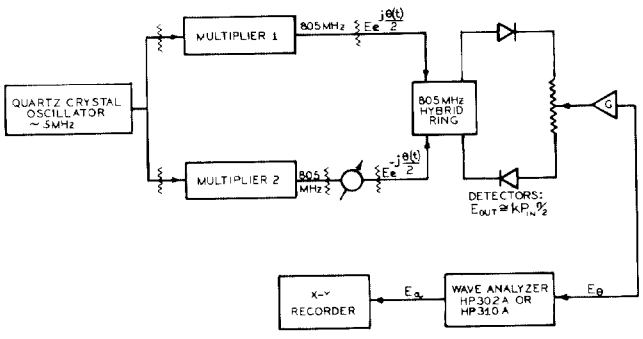


Fig. 5. Measurement method used to determine the spectral density,  $S_{\theta}(\omega)$ , of phase fluctuations in the output of a stable rf phase reference generator.

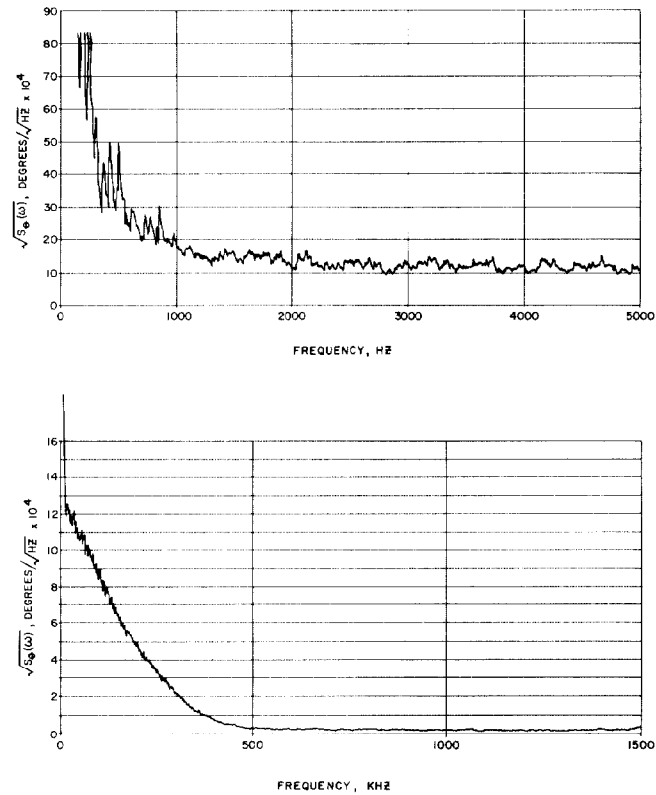


Fig. 6. Phase fluctuation spectral density,  $S_{\theta}(\omega)$ , of the 805-MHz output of an experimental reference source using a vacuum tube multiplier chain.  $\xi = 0.0365$  V/deg. Upper trace taken with Hewlett-Packard 302A analyzer,  $\Delta f_{1/2} = 3.5$  Hz. Lower trace taken with Hewlett-Packard 310A analyzer,  $\Delta f_{1/2} = 108$  Hz. Background from measurement system with phase bridge inputs shorted or autocorrelating input from one multiplier was less than  $10 \mu\text{V}$ , or  $2 \times 10^{-5}$  deg/ $\sqrt{\text{cps}}$ .